Production of Λ hyperons in 4.0 AGeV and 4.5 AGeV carbon-nucleus interactions at the Nuclotron

for BM@N Collaboration

April, 2025

Abstract

The BM@N experiment (Baryonic Matter at the Nuclotron) is the first experiment undertaken at the JINR NICA-Nuclotron accelerator complex. The BM@N scientific program comprises studies of dense nuclear matter in heavy ion beams of the intermediate energy range between the SIS-18 and NICA/FAIR facilities. In this paper the results of the analysis of data are collected with the carbon beam at the 4.0 and 4.5 AGeV kinetic energy interacting with the different solid targets (C, Al, Cu, Pb). Transverse momentum, rapidity spectra and yields of Λ hyperons are measured. The results are compared with the theoretical models predictions and with the experimental data on carbon-carbon interactions measured at lower energies.

1 Introduction

The study of relativistic heavy-ion collisions provide a unique opportunity to explore nuclear matter under extreme conditions of density and temperature. The optimal energy range for the nuclear matter compression is close to 5 AGeV. The Nuclotron at NICA accelerating complex provide a wide range of ion beams within the energy range $\sqrt{s_{NN}} = 2.3 - 3.5$ GeV. These energies are high enough for strange mesons and (multi)-strange hyperons production in nucleus-nucleus collisions close to the kinematic threshold [1, 2].

Λ hyperons containing a single strange quark are important observables in the study of strangeness because their kinematic characteristics carry information about the dynamics of the system, the degree of thermalisation and the role of secondary interactions.

The production of Λ hyperons at low and intermediate energies has been studied in a number of experiments, notably FOPI (GSI) [4] and HADES (GSI) [5]. The HADES and FOPI experiments have provided detailed spectra of hyperons in symmetric systems such as $Ni + Ni$, $Ar + KCl$, etc., but the range of nuclear masses and energies covered by them does not always include light and asymmetric systems.

In addition, data on Λ hyperons have been obtained in the STAR (RHIC) [6] and ALICE (LHC) [7] collider experiments, but in these experiments the focus is on the central fast region and significantly higher energies. In contrast, the fixed-target experiments allow us to study both the central and front regions, which is particularly important for analyses of asymmetric systems and low energies. The BM@N experiment is the first fixed-target experiment operated at the NICA accelerating complex. The BM@N experiment collected data on carbon, argon, krypton and xenon beams with different solid targets. Recently the results on $\pi+$ and K$+$ mesons in argon-nuclear collisions were published in [8].

This paper presents results of the Λ hyperon production in carbon-nucleus interactions (CN run) at the 4.0 and 4.5 AGeV beam kinetic energies. Transverse momentum, rapidity spectra and yields of the Λ hyperons are measured. The results are compared with theoretical models predictions and with the experimental data on carbon-carbon interactions. The structure of the paper is organised as follows:

Section 2 describes the BM@N experimental setup and the detector configuration used;

Section 3 describes the details of MC modeling and evaluating the efficiency of triggers.

Sections 5, 6 and 4 presents the analysis methodology and the event selection procedure;

Section 7 describes the procedure for the evaluation of the cross section and yields in the BM@N acceptance region. The estimation of the systematic error is given in this section.

Section 8 presents the inverse spectra of p_T from the fitting of which the temperature T_0 and rapidity distributions were obtained. The experimental measurement results are compared with the predictions of the DCM-SMM, UrQMD and PHSD models.

Section 9 presents all final measurement results (yields, slopes T_0, cross sections). The results are compared with model predictions. The results of the C + C interaction are compared with measurements in a Propane Chamber (Dubna).

2 Experimental setup configuration

The experimental run of the BM@N spectrometr was performed with the carbon beam with the different targets: C, Al, Cu, Pb. The research program was devoted to measurements of inelastic reactions $C + A \to X$ with beam kinetic energy of 4.0 and 4.5 AGeV. The BM@N setup in CN run is shown in Fig. 1.

The data from the central tracker, outer drift chambers (DCH), time-of-flight detectors (ToF), zero degree calorimeter (ZDC), trigger system T_0T and beam detectors were collected using the integrated data acquisition system. The configuration of the central tracker was based on one plane of a forward silicon detector (Si) with double-side readout, six two-coordinate GEM (Gaseous Electron Multiplier) stations combined from five GEM detectors with the size of 66x41 cm^2 and two GEM detectors with the size of 163x45 cm^2 [11].

The tracking stations were arranged to have the beam passing through their centers. Each successive GEM station was rotated by 180^o around the vertical axis. It was done to have the opposite electron drift direction in the successive stations in order to avoid a systematic shift of reconstructed tracks due to the Lorentz angle in the magnetic field. A technical description of the BM@N spectrometer is given in [9, 10].

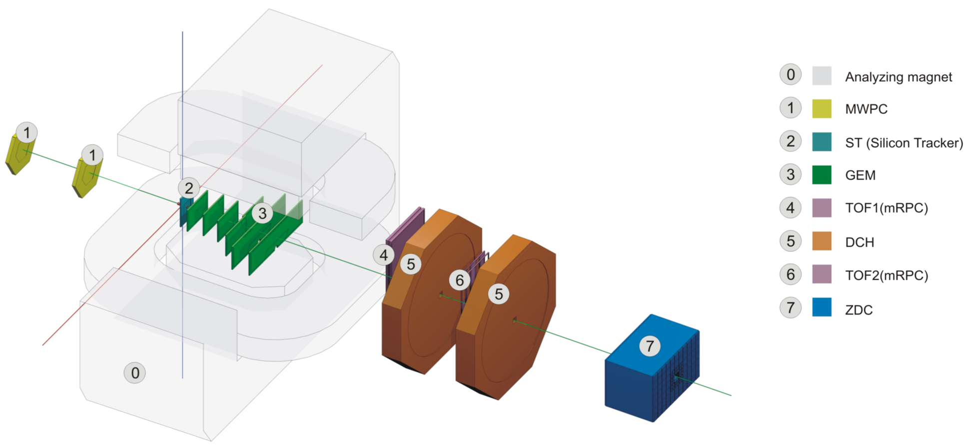

Figure 1: Scheme of the BM@N setup in the CR run.

The technical part of the run included the measurement of the carbon beam momentum and its resolution in the central and outer trackers at different values of the magnetic field. In addition, experimental data on the minimum bias interactions of the beam with different targets were analyzed in order to reconstruct tracks, primary and secondary vertices using central tracking detectors [12–14]. Since the GEM tracker configuration was tuned to measure relatively high-momentum beam particles, the geometric acceptance for relatively soft decay products of strange V0 (Λ, K^0_S) particles was rather low (few percent).

In the present analysis the experimental data from the forward Si detector, GEM detectors, trigger barrel multiplicity detector (BD), beam counter (BC2), veto (VC) and T0 counters were used (Fig. 2).

The carbon beam intensity was few 10^5 per the spill, the spill duration was 2.0-2.5 sec. The magnetic field in the center of the analyzing magnet was 0.61 T. To form a minimum bias trigger signal a hit multiplicity in the BD detector situated around the target was required to be $N_{BD} \geq 2$ for the carbon target (C) and $N_{BD} \geq 3$ for the Al, Cu, Pb targets. The analyzed physical data statistics of the carbon-nucleus collisions were 13 M and 16 M events for 4.0 AGeV and 4.5 AGeV energy beam, respectively.

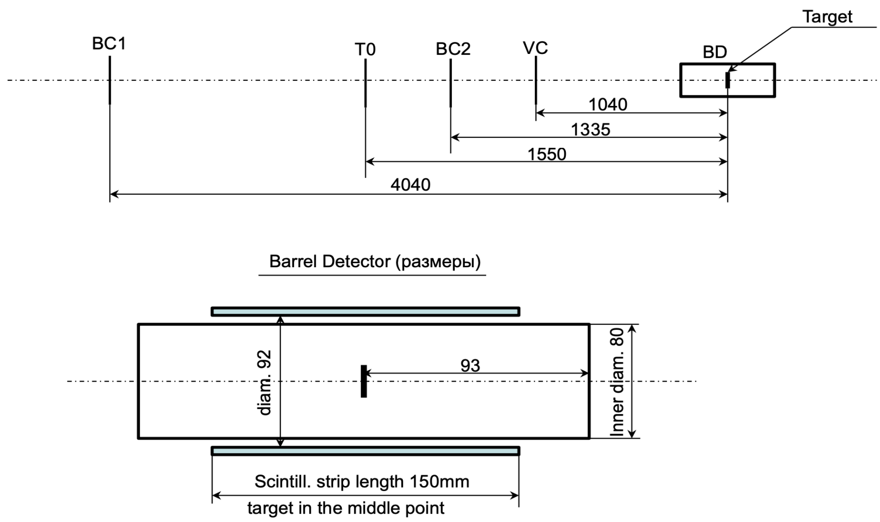

Figure 2: Schematic view of the beam counters, barrel detector and target positions. Target was installed inside the barrel detector.

3 Monte Carlo simulation

Monte Carlo event samples of $C + A$ collisions were produced with the DCM-QGSM event generator [19, 20]. The transportation of particles through the setup volume was simulated with the GEANT3 program [21] integrated into the BmnRoot software framework [22]. The GEM detectors response in the magnetic field was simulated with the micro-simulation package Garfield++ [23].

The package gives detailed description of the processes inside the GEM detector, including the drift and diffusion of released electrons in electric and magnetic fields and the electron multiplication in GEM foils, so that the output signal from the readout plane can be well reproduced. To speed up the simulation, the dependencies of the Lorentz shifts and the charge distributions on the readout planes were parameterized and used in the GEM digitization part of the BmnRoot package. The details of the detector alignment and Lorentz shift corrections are described in the paper [24].

Trigger efficiency ϵ_{trig} was calculated from the trigger BD detector multiplicity distributions produced by a convolution of the reconstructed Λ hyperons and delta electrons events which were found to be the dominant source using GEANT3 simulated events for the $C + A$ processes. It was evaluated in the range between $80 \pm 2\%$ for $C + C$ and $95 \pm 2\%$ for $C + Pb$ minimum bias interactions.

The systematic errors of ϵ_{trig} cover:

1) the contribution of delta electrons background produced in the simulated targets with the fractional thickness from 0.5 to 1.0 of the real targets;

2) the spread of the trigger efficiency values for the reconstructed Λ hyperons calculated for a different y and p_T bins;

3) changes in the trigger efficiency after adjustment (reweighting) of the simulated track multiplicity to the experimental distributions. The trigger efficiency obtained in the simulation was confirmed by the analysis of the data samples with the reduced trigger requirements.

4 Event selection

The track reconstruction method was based on the so-called "cellular automaton" approach [15]. Λ hyperons events were reconstructed using "V_0" decay topology, where an unobserved strange particle decays into two observed charged daughter particles. Events with Λ decay mode into (p, π^-) pairs were selected.

Since the particle identification was not used in this analysis all positive tracks were considered as protons and all negative as π^-. Λ hyperon selection criteria were the following:

- Each track has at least 4 hits in GEM detectors (6 stations in total), where hit is a combination of two strip clusters on both readout sides (X and X' views) on each detector [11]
- Momentum range of the positive tracks is limited to $p_{pos} < 3.9(4.4)$ GeV/c for 4.0 (4.5) AGeV carbon beam data to remove tracks from the beam spot
- Momentum range of negative tracks: $p_{neg} > 0.3$ GeV/c
- Distance of the closest approach of the V_0 decay tracks (distance in X-Y plane between V_0 decay tracks at Z_{V0}) : dca < 1.0 cm
- Distance between the V_0 decay vertex and primary vertex: path > 2.5 cm

The signal from Λ hyperon decays is observed as a narrow peak in the invariant mass distribution of the two tracks with opposite charge with the proton and pion mass hypothesis Fig. 3.

Signal evaluation in Monte Carlo and Data follows the same procedure. The peak region within $\pm 3 \cdot \sigma$ was excluded from the fit. Here σ corresponds to the width of the peak. The rest of the distibution was fit with the convolution of the threshold and exponential functions:

$$f_{\text{bg}}(m) = N(m - M_0)^A \cdot \exp\left[-B(m - M_0)\right],$$

with N, A , B as a free parameters of the fit function; m is the running invariant mass and M_0 = 1.078 GeV is the threshold limit.

The signal value is the summ of the bin contents within the peak region after the background subtraction.

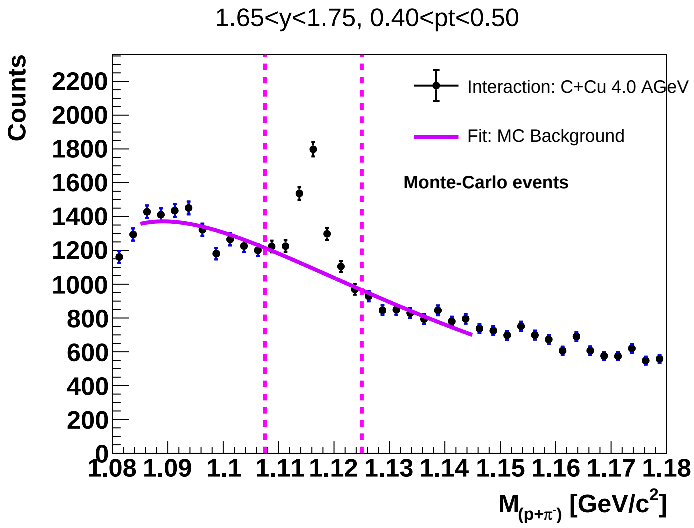

Figure 3: MC invariant mass spectra of (p, π^-) pairs reconstructed in interactions of the 4.0 AGeV carbon beam with the Cu target. The violet lines represent the result of the fit by the sum of the threshold and exponential functions. The vertical lines show the mass window in which the Λ signal is calculated as an excess of the histogram relative to the background.

5 Acceptance evaluation

The acceptance evaluation procedure was performed using the DCM-QGSM model data generated for the C beam with C, Al, Cu, Pb targets at the 4.0 and 4.5 AGeV energies.

The $1.2 < y < 2.1$ and $0.1 < p_T < 1.05$ GeV/c analyzed kinematic range was divided into 8×8 cells [25]. For each cell the signal was evaluated follow the procedure described in the previous section.

The acceptance value ω_{acc} was calculated as the ratio of the number of reconstructed Λ hyperons to the number of generated ones in the (y, p_T) intervals: ω_{acc}= N$_{rec_{MC}}$/N$_{gen_{MC}}$.

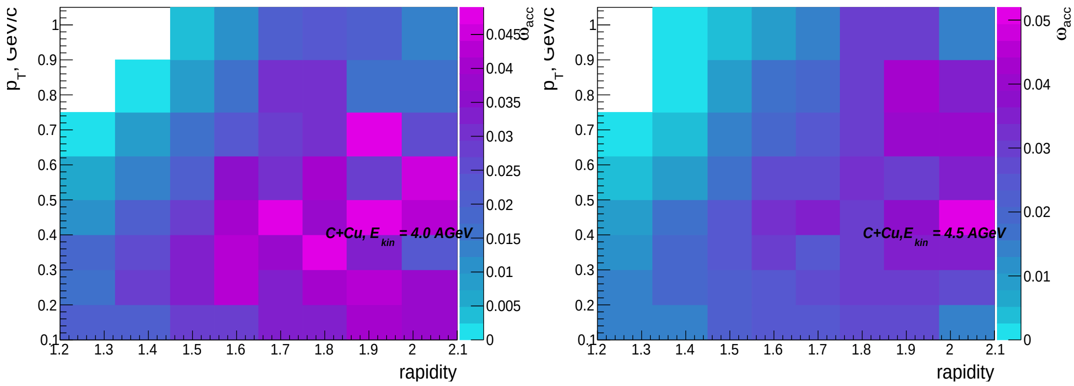

Figure 4: The acceptance distributions of the $C + Cu$ interactions for the 4.0 (left) and 4.5 AGeV (right) energies.

The possible variation of the acceptance values was done by bootstrapping method. Each invariant mass distribution was resampled 1000 times, each time the signal value was calculated and filled the histogram. These accumulated histogram was fit by the Gaussian function and the σ of the fit was used as an uncertainty of the acceptance value.

The distributions of the calculated acceptance values in the analyzed (y, p_T) kinematic region are shown in Fig. 3. The white empty areas indicate cells with low efficiencies due to the low statistic. All these cells with efficiencies below the < 0.01 threshold were excluded from the analysis. The extrapolation procedure was performed for these cells to obtain the number of expected events according to the model.

The extrapolation factor f_{extrap} was calculated as a ratio of the number of MC generated Λ hyperons in the cells along p_T column to the number of the reconstructed Λ hyperons with the reconstruction efficiency above $\omega_{acc_i} > 0.01$ in this column.

6 Data analysis

For each reconstructed event in the experimental data the reconstruction efficiency value ω_{acc} was assigned according to the kinematic region (y, p_T) which this event belongs. The invariant mass distributions of (p,π^-) pairs were obtained for each (y, p_T) cell with a weight of $1/\omega_{acc}$.

The invariant mass distributions of p and π^- for reconstructed interactions of the 4.5 AGeV carbon beam with the C, Al, Cu, Pb targets are shown in Fig. 5. The background part of the distributions was fitted using a combination of the threshold and exponential functions (see Chapter 4) in the 1.085-1.145 GeV/c^2 mass region. In the 1.1075 - 1.125 GeV/c^2 mass window the Λ signal was excluded from the fit. The number of reconstructed Λ was calculated according to the formulae: $N_{sig} = N_{hist} - N_{bg}$. The error of the Λ signal includes the uncertainty of the background subtraction. The approach for the statistical uncertainty evaluation in the experimental data was the same as in the Monte-Carlo simulation (Chapter 5).

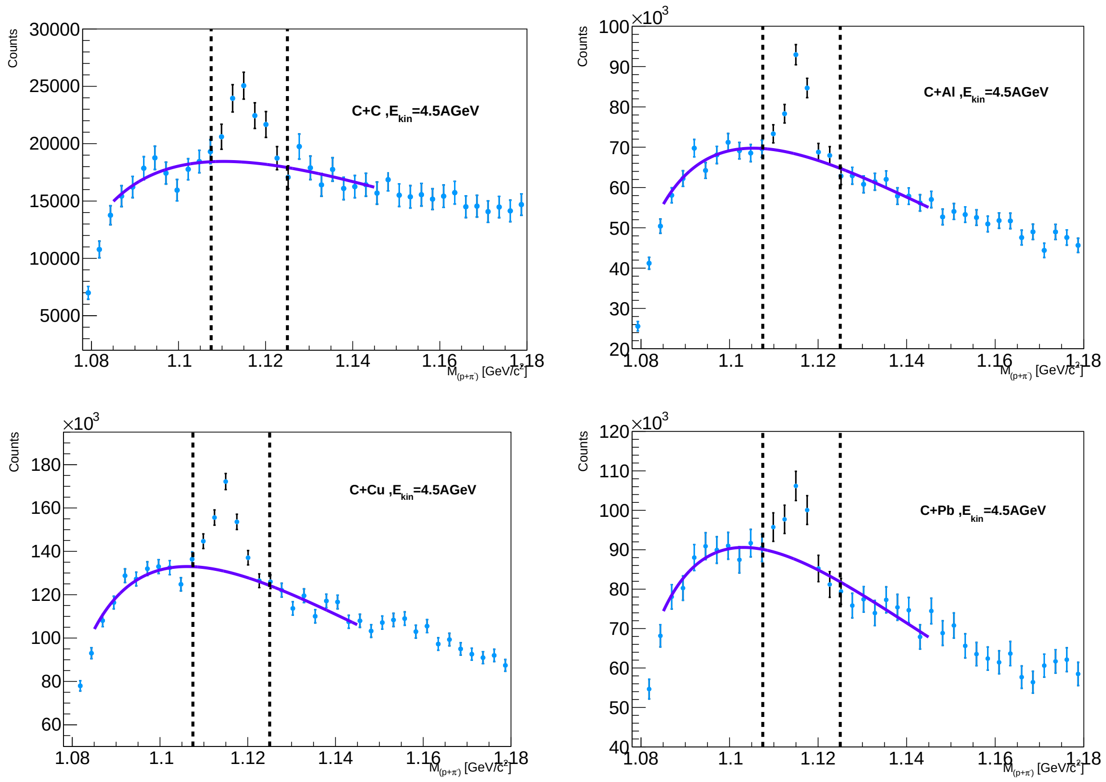

Figure 5: Invariant mass spectra of (p, π^-) pairs reconstructed in interactions of the 4.5 AGeV carbon beam with the C, Al, Cu, Pb targets. The violet lines represent the result of the fit by the sum of the threshold and exponential functions. The vertical lines show the mass window in which the Λ signal is calculated as an excess of the histogram relative to the background.

7 Evaluation of Λ hyperon cross sections and yields

The inclusive cross section σ_Λ and the yield Y_Λ of Λ hyperon production in $C+C$, $C+Al$, $C+Cu$, $C+Pb$ interactions were calculated in y (p_T) bins according to the formulae:

$$\sigma_\Lambda(y) = \sum_{p_T} \left[\frac{N_\Lambda(y, p_T)}{\epsilon_{\text{rec}}(y, p_T) \cdot \epsilon_{\text{trig}} \cdot L} \right], \quad Y_\Lambda(y) = \frac{\sigma_\Lambda(y)}{\sigma_{\text{inel}}},$$
$$\sigma_\Lambda(p_T) = \sum_{y} \left[\frac{N_\Lambda(y, p_T)}{\epsilon_{\text{rec}}(y, p_T) \cdot \epsilon_{\text{trig}} \cdot L} \right], \quad Y_\Lambda(p_T) = \frac{\sigma_\Lambda(p_T)}{\sigma_{\text{inel}}},$$

where L is the luminosity, N_Λ is the number of reconstructed Λ hyperons, ϵ_{rec} is the combined efficiency of the Λ hyperon reconstruction, ϵ_{trig} is the trigger efficiency, σ_{inel} is the cross section of the inelastic $C+A$ interactions. The cross section for inelastic $C+C$ interactions is taken from the measurement [28].

The cross sections for inelastic $C+Al$, $C+Cu$, $C+Pb$ interactions are taken from the predictions of the DCM-QGSM model which are consistent with the results calculated by the formula:

$$\sigma_{inel} = \pi R_0^2 \left(A_P^{1/3} + A_T^{1/3} \right)^2,$$

where $R_0 = 1.2$ fm is the effective nucleon radius, and A_P and A_T are the atomic mass numbers of the projectile and target nuclei, respectively [31].

The uncertainties for $C+Al$, $C+Cu$, $C+Pb$ inelastic cross sections are estimated from the alternative formula:

$$\sigma_{inel} = \pi R_0^2 \left(A_P^{1/3} + A_T^{1/3} - b \right)^2,$$

with $R_0 = 1.46$ fm and $b = 1.21$ [28].

The values and uncertainties of σ_{inel} for $C+C$, $C+Al$, $C+Cu$, $C+Pb$ interactions used to evaluate the Λ hyperon yields are given in Table 1.

The yields of Λ hyperons in minimum bias $C+C$, $C+Al$, $C+Cu$, $C+Pb$ interactions are measured in the kinematic range on the Λ hyperon transverse momentum $0.1 < p_T < 1.05$ GeV/c and the Λ hyperon rapidity in the laboratory frame $1.2 < y < 2.1$ for 4 AGeV and 4.5 AGeV data.

The main sources of systematic uncertainty that contribute to the Λ hyperon yields can be characterized as follows:

- Statistical fluctuations in Monte Carlo and experimental data

  To evaluate the statistical fluctuations of the signal each bin of the reconstructed mass spectra distributions was smeared according to the Gaussian function, where the mean parameter corresponded to the bin value and sigma parameter corresponded to the statistical error. The varied signal distributions were fitted using Gaussian function and $\sigma_{N_{rec_{MC}}}$ and $\sigma_{N_{rec_{DATA}}}$ values were extracted from the fits. The systematic uncertainty from this source was estimated as:

$$\delta Y_{\Lambda_{pseudoexp}} = Y_{\Lambda} \sqrt{\sigma^2_{N_{rec_{DATA}}} / N^2_{rec_{DATA}} + \sigma^2_{N_{rec_{MC}}} / N^2_{rec_{MC}}},$$

where $N_{rec_{MC}}$ and $N_{rec_{DATA}}$ the values of the reconstructed Λ hyperons in the MC and experimental data, respectively.

- Uncertainties due to selection cut criteria

  To estimate the systematic error from this source a series of analyzes were performed with the different values of the "path" and "dca" selection parameters. The values variations of these parameters were performed within ±10% of the values used in the analysis (Chapter 4). The maximal deviation of the calculated Λ yield values was 20% and the systematic uncertainty from the cut variation analyzes was estimated as $\delta Y_{\Lambda_{cutvar}}$ = 0.004.

- The total systematic error was calculated as:

$$\delta Y_{\Lambda_{total}} = \sqrt{(\delta Y^2_{\Lambda_{pseudoexp}} + \delta Y^2_{\Lambda_{cutvar}})}$$

8 Rapidity and p_T spectra

The rapidity of the beam-target nucleon-nucleon CM system calculated for an interaction of the carbon beam with of 4.0 (4.5) AGeV kinetic energy with a fixed target is $y_{CM} = 1.17(1.22)$. The Λ hyperon rapidity range for 4.5 AGeV data is shifted at +0.05 to get approximately the same y^* range in the CM system as for 4.0 AGeV data. The transformation of the y distribution from the laboratory system to c.m.s. gives $y^* = y - y_{CM}$.

The differential spectra of the Λ hyperon yields in y are measured in the Λ hyperon transverse momentum range $0.1 < p_T < 1.05$ GeV/c. The differential y spectra of the Λ hyperon yields corrected to the detector acceptance and efficiency are presented in Fig. 6.

The invariant differential Λ hyperons yields as a function of the p_T are presented on Fig. 7 and fitted by the function:

$$\frac{1}{p_T} \cdot \frac{d^2N}{dp_T\, dy} \propto \exp\left(-\frac{m_T - m_\Lambda}{T_0}\right),$$

where $m_T = \sqrt{m_\Lambda^2 + p_T^2}$ is the transverse mass, the inverse slope parameter T_0 is a free parameter of the fit, dy corresponds to the measured y range.

The predictions of the DCM-SMM [19, 20], UrQMD [26] and PHSD [27] models are shown for comparison.

The inverse slope T_0 values were extracted from the fit of the invariant p_T spectra and summarized in Tables 1, 2 for 4.0 AGeV and 4.5 AGeV carbon beam data respectively.

The fit results are consistent within the uncertainties with the predictions of the DCM-SMM, UrQMD and PHSD models. In general, the models considered describe the shape of the differential spectra in y^* and p_T, but predict more abundant yields of Λ hyperons than measured in the experiment.

The predictions of DCM-SMM and UrQMD models are closer to the experimental data than the predictions of the PHSD model. The PHSD model predicts a stronger increase in Λ hyperon yield in the BM@N kinematic range with an increasing atomic weight of the target than the DCM-SMM and UrQMD models.

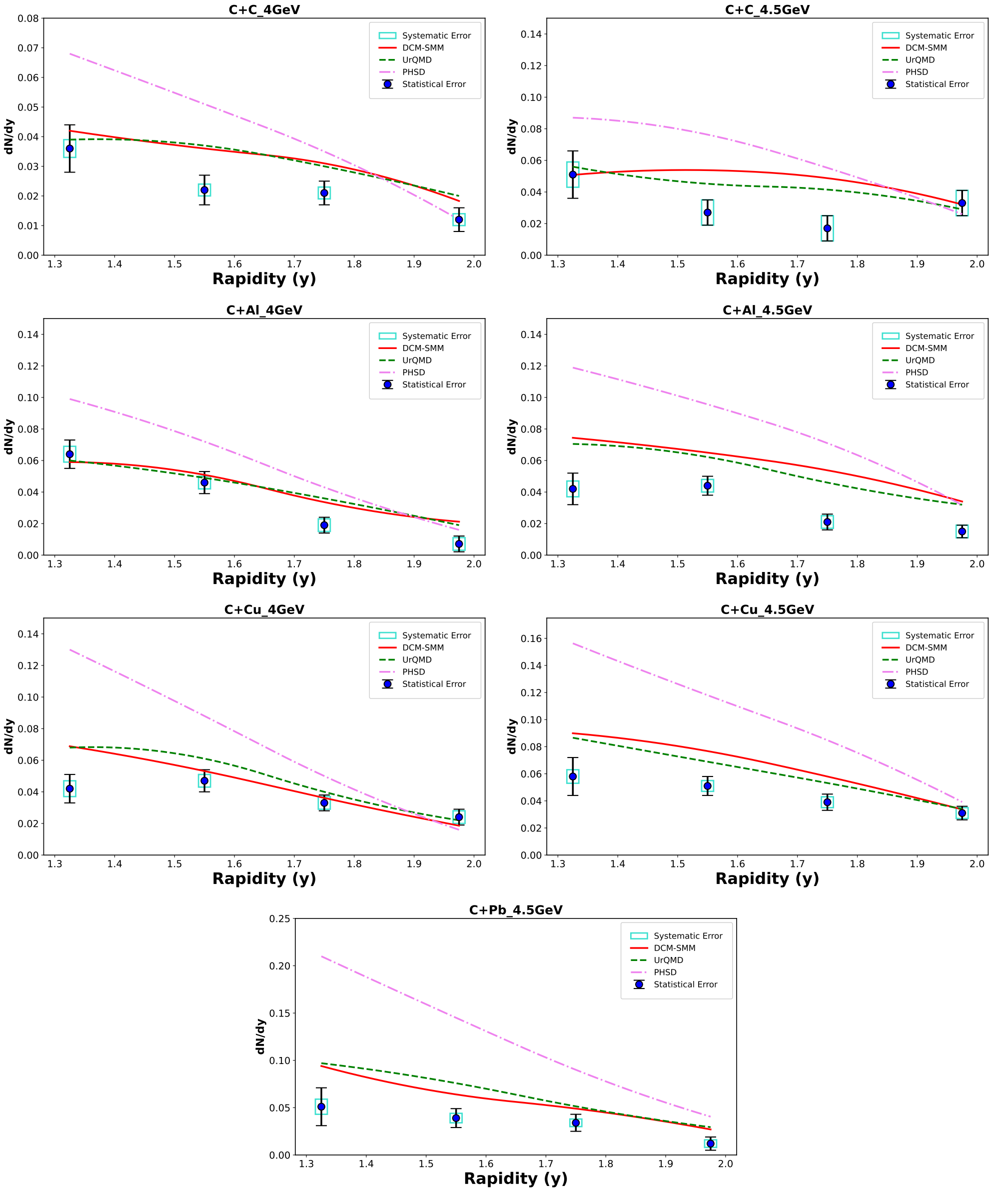

Figure 6: Rapidity y spectra of Λ hyperons produced in $C+C$, $C+Al$, $C+Cu$ interactions with the carbon beam energy of 4.0 AGeV (left plots) and 4.5 AGeV (right plots). Bottom plot corresponds to $C+Pb$ reaction at 4.5 AGeV. The error bars represent the statistical errors, the blue boxes show the systematic errors. The predictions of the DCM-SMM, UrQMD and PHSD models are shown as colored lines.

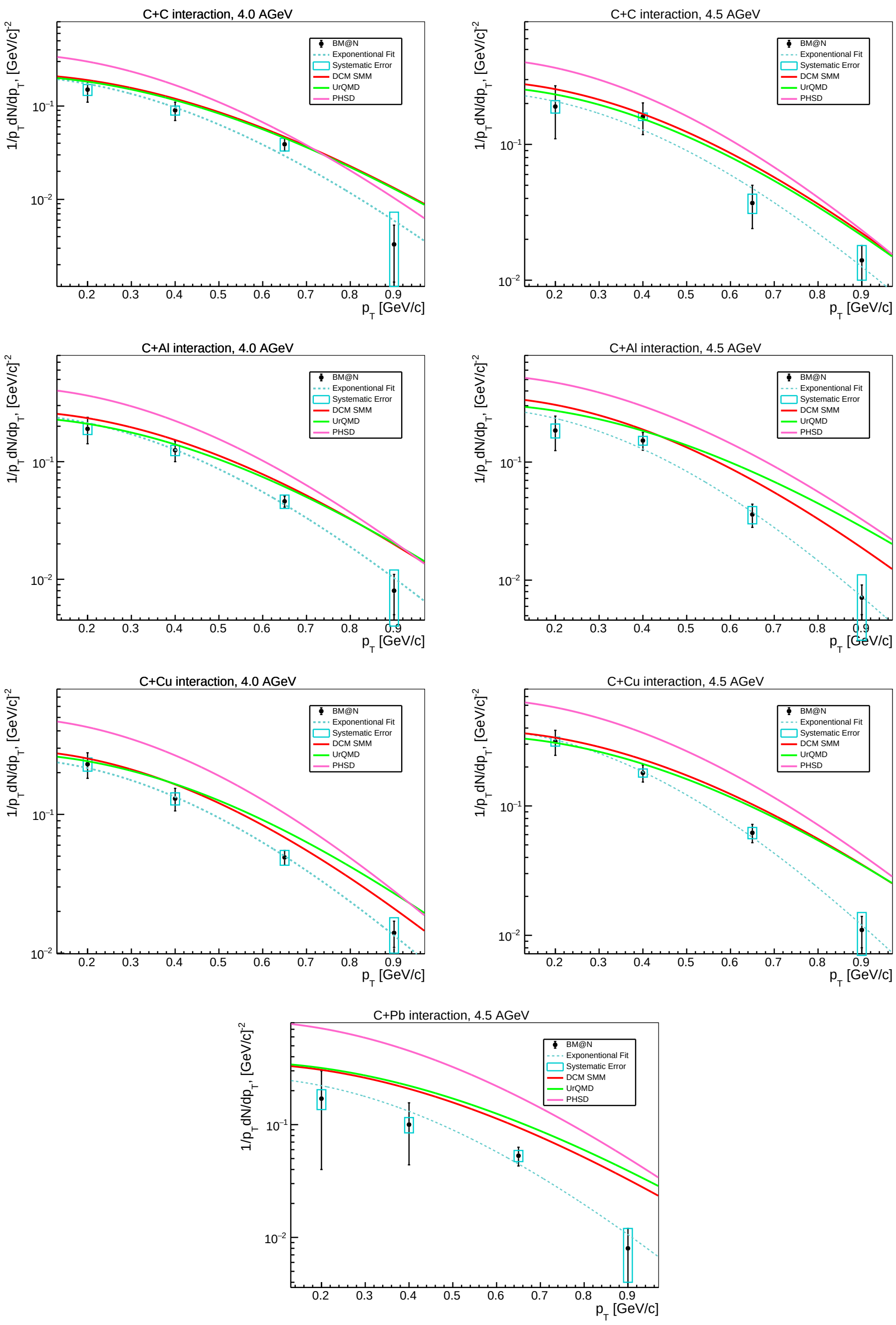

Figure 7: Invariant transverse momentum p_T spectra of Λ hyperons produced in $C + C$, $C + Al$, $C + Cu$ interactions with the carbon beam energy of 4.0 AGeV (left plots) and 4.5 AGeV (right plots). Bottom plot corresponds to $C + Pb$ reaction at 4.5 AGeV. The error bars represent the statistical errors, the blue boxes show the systematic errors. The blue lines represent the results of the parameterization described in the text. The predictions of the DCM-SMM, UrQMD and PHSD models are shown as colored lines.

9 Results

The Λ yields, cross sections and inverse slope parameters T_0 for $C+C$, $C+Al$, $C+Cu$, $C+Pb$ interactions are summarized in Tables 1 and 2.

The measured Λ yields within BM@N acceptance were extrapolated to the full kinematic range. The extrapolation factor values were calculated as the average predictions of the DCM-SMM and UrQMD models. The calculated Λ yields in full kinematic region and the extrapolating factor values are presented in Tables 1, 2. In Fig. 8 the Λ yields in the full kinematic region are shown in dependence on the kinetic energy of the carbon beam.

Table 1: Λ hyperon yields, cross sections and p_T spectra slope parameters in minimum bias 4.0 AGeV $C+C$, $C+Al$, $C+Cu$ interactions. The first error given is statistical, the second error is systematic.

4 AGeV Carbon beam	C+C	C+Al	C+Cu	C+Pb
Measured Λ yield $/10^{-2}$	$2.3 \pm 0.3 \pm 0.5$	$3.2 \pm 0.4 \pm 0.6$	$3.0 \pm 0.3 \pm 0.5$	low statistics
Extrap. factor average	2.49 ± 0.18	3.01 ± 0.13	4.0 ± 0.06	6.72 ± 0.44
Full Λ yield N_Λ $/10^{-2}$	$5.7 \pm 0.7 \pm 1.0$	$9.6 \pm 1.0 \pm 2.0$	$12.0 \pm 1.0 \pm 2.0$	low statistics
N_{part}, DCM-SMM	9.0	13.4	23.0	50.5
N_{part}, UrQMD	7.2	11.4	19.3	50.0
N_{part}, PHSD	8.4	11.9	17.3	30.8
$N_\Lambda/N_{part}/10^{-3}$	$6.3 \pm 0.08 \pm 0.1$	$7.2 \pm 0.8 \pm 1.5$	$5.70 \pm 0.39 \pm 0.30$	———
Λ cross section, mb	$47.3 \pm 5.8 \pm 8.3$	$121.0 \pm 15.1 \pm 22.7$	$214.8 \pm 21.5 \pm 35.8$	
σ_{inel}, mb	830 ± 50 [28]	1250 ± 50 [31]	1790 ± 50 [31]	3075 ± 50 [31]
Inverse slope T_0, MeV	$89 \pm 9 \pm 17$	$99 \pm 10 \pm 16$	$108 \pm 11 \pm 14$	

Table 2: Λ hyperon yields, cross sections and p_T spectra slope parameters in minimum bias 4.5 AGeV $C+C$, $C+Al$, $C+Cu$, $C+Pb$ interactions. The first error given is statistical, the second error is systematic.

4.5 AGeV Carbon beam	C+C	C+Al	C+Cu	C+Pb
Measured Λ yield $/10^{-2}$	$2.7 \pm 0.5 \pm 0.6$	$2.5 \pm 0.3 \pm 0.5$	$3.7 \pm 0.4 \pm 0.6$	$3.3 \pm 0.1 \pm 0.1$
Extrap. factor average	2.34 ± 0.08	2.88 ± 0.16	3.76 ± 0.15	6.24 ± 0.14
Full Λ yield N_Λ $/10^{-2}$	$6.3 \pm 1.2 \pm 1.4$	$7.1 \pm 0.9 \pm 1.4$	$14.0 \pm 2.0 \pm 2.0$	$20.0 \pm 6.0 \pm 6.0$
$N_\Lambda/N_{part}/10^{-3}$	$7.0 \pm 0.13 \pm 0.16$	$5.3 \pm 0.7 \pm 1.0$	$6.08 \pm 0.86 \pm 0.86$	$3.8 \pm 1.1 \pm 1.1$
Λ cross section, mb	$52.5 \pm 9.7 \pm 11.6$	$90.7 \pm 11.3 \pm 18.1$	$249.0 \pm 35.8 \pm 40.3$	$633.2 \pm 191.9 \pm 191.9$
Inverse slope T_0, MeV	$107 \pm 17 \pm 17$	$86 \pm 8 \pm 17$	$91 \pm 8 \pm 15$	$99 \pm 17 \pm 20$

The BM@N results are compared with the predictions of the DCM-SMM, UrQMD and

PHSD models (Fig. 8). The tendency of the Λ hyperon yields to increase with increasing energy is observed. In general, the model predictions exceed the experimental data. The PHSD model predicts higher full yields of the Λ hyperons than the other two models.

The Λ hyperon yields and production cross sections in $C + C$ interactions can be compared with the BM@N result 47.3 ± 5.8 mb and 24.0 ± 6.0 mb measured in the carbon beam interactions with the momentum of 4.2 GeV/c per nucleon (the beam kinetic energy of 3.36 AGeV) in the Propane Chamber experiment [29, 30]. On Fig. 8 (top left) the BM@N results for the Λ hyperon yields in $C+C$ minimum bias interactions are compared with the results taken from the Propane Chamber experimental data analysis.

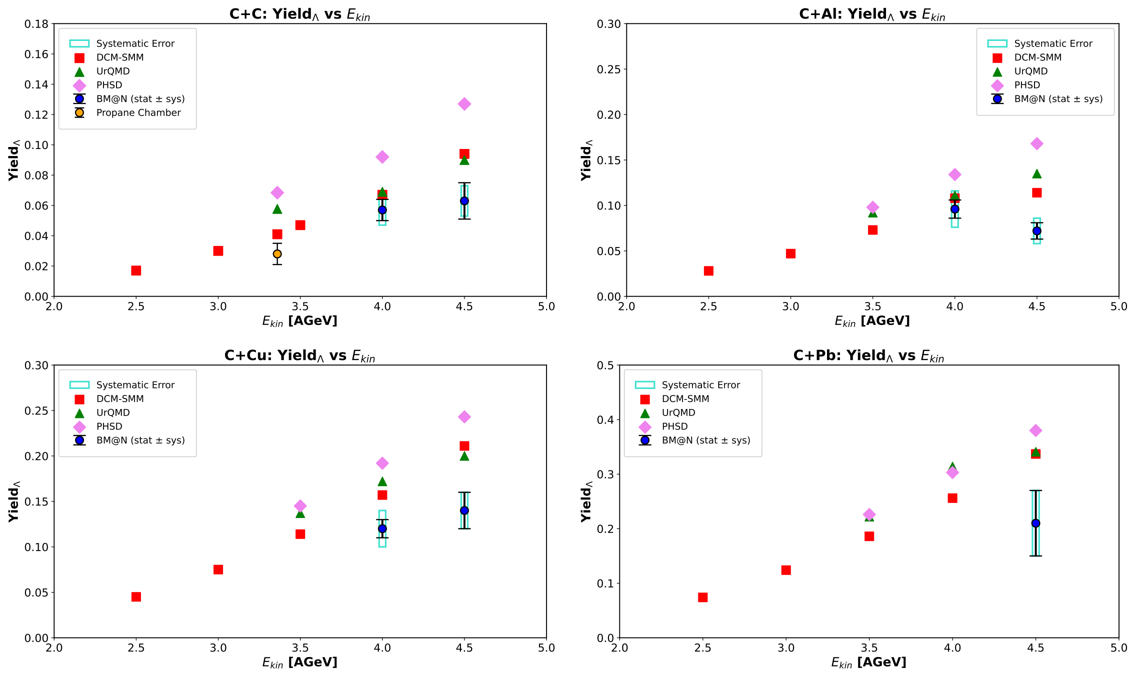

Figure 8: Energy dependence of Λ hyperon yields in minimum bias $C + C$, $C + Al$, $C + Cu$, $C + Pb$ interactions. The BM@N error bars represent the statistical errors, the blue rectangles show the systematic errors. The BM@N results for $C + C$ interactions are compared with the experimental data taken from [29, 30]. The predictions of the DCM-SMM, UrQMD and PHSD models are shown as colored points.

The calculated Λ hyperon yields in full kinematic region for the $C + C$ collisions were compared with a parameterization model developed for proton-proton ($p + p$) interactions and scaled to the $C + C$ system.

The parameterization model is based on the Lund String Model (LSM) [32] and is expressed as:

$$\langle n_{pp} \rangle = a(x - 1)^b x^{-c},$$

where $x = s/s_0$ is the square of the center-of-mass energy, s_0 is the square of the production threshold and a, b, c are the fit parameters from [33].

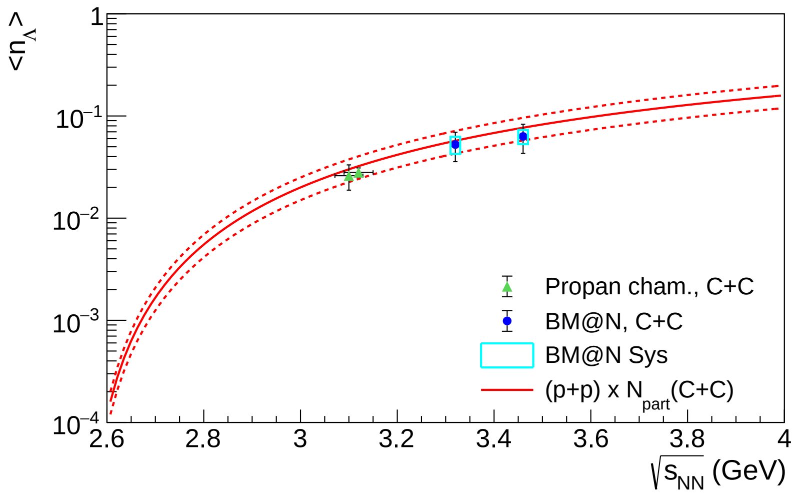

Figure 9: The integrated yield of Λ hyperons in $C + C$ collisions as a function of $\sqrt{s_{NN}}$. BM@N experimental data are compared with a parameterization model based on pp collisions scaled to the $N_{\text{part}} = 9$. Dashed red lines indicate the uncertainties in the predicted excitation function (about 25%).

Since $C + C$ includes not only $p + p$ but also $p + n$ and $n + n$ interactions, and near-threshold of Λ yields are about 25% lower in $n + n$ and $n + p$ compared to $p + p$ [34], the isospin correction factor was calculates as:

$$k_{\text{iso}} = f_{pp} \cdot \alpha + (f_{np} + f_{pn} + f_{nn}) \cdot \beta,$$

with $\alpha = 1.0$ for $p+p$ and $\beta = 0.75$ for $n+n$, $n+p$, and $p+n$ collisions. The fractions f_{ij} are determined by the composition of nucleons in the colliding carbon nuclei.

The total yield $\langle n_\Lambda \rangle$ for $C + C$ was scaled as:

$$\langle n_\Lambda \rangle = \langle n_{pp} \rangle \cdot k_{\text{iso}} \cdot N_{\text{part}},$$

where N_{part} is the number of the participating nucleons and k_{iso} is the isospin correction factor.

The BM@N results for the Λ yields in the $C + C$ collisions at 4.0 and 4.5 AGeV are in good agreement with the scaled $p + p$ parameterization model (Fig. 9). The parameterization provides a reliable basis for the estimation of Λ hyperon production in carbon-carbon interactions. The agreement with the BM@N experimental data supports its applicability for light-symmetric systems. In addition, the number of participating nucleons N_{part} used in the scaling was taken from the DCM-SMM model and it was evaluated according to existing measurements from the Propane Chamber experiment.

To compare yields of particle production in nucleus-nucleus interactions, they are usually normalized to the number of nucleon participants. For the DCM-SMM, UrQMD, PHSD models the number of participants in the reactions $C + A$ was calculated (Tab. 1). For the both energies 4.0 AGeV and 4.5 AGeV obtained N_{part} values are the same.

The integrated Λ hyperon yields for each model were normalized to the corresponding number of participants N_{part}. The experimental data were normalized to the N_{part} values obtained for the DCM-SMM model. The ratios of the Λ hyperon yields to the number of nucleons participants measured by BM@N are given in Tables 1 and 2. Comparison of experimental data with the predictions of the DCM-SMM, UrQMD and PHSD models for 4.0 AGeV and 4.5 AGeV carbon nucleus interactions is shown in Fig. 10.

There is a tendency that the measured ratios are smoothly decreasing for heavier target nuclei. This tendency is also predicted by the models.

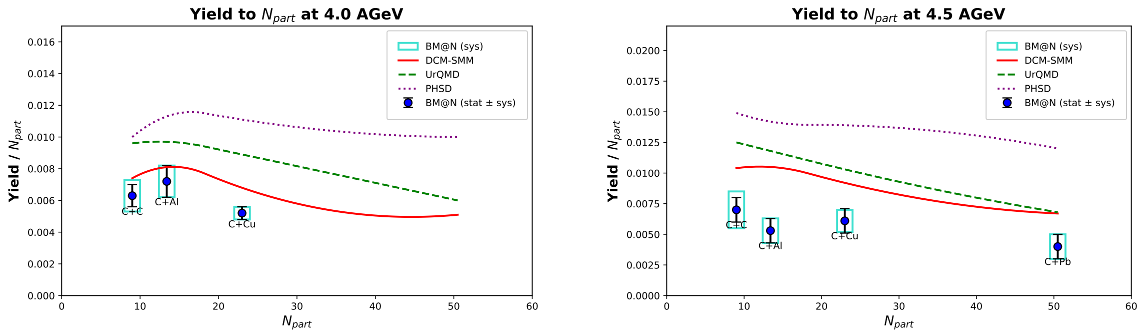

Figure 10: Ratios of the Λ hyperon yields to the number of nucleons-participants measured by BM@N in minimum bias carbon-nucleus interactions at 4.0 AGeV (left) and 4.5 AGeV (right). Error bars show statistical uncertainties, while blue rectangles indicate systematic errors. The predictions of the DCM-SMM, UrQMD and PHSD models are shown in colored lines.

10 Summary

The production of Λ hyperons in the interactions of the carbon beam with the *C*, *Al*, *Cu*, *Pb* targets was measured with the BM@N detector. The physical results of the BM@N experiment are presented on the Λ hyperon yields and cross sections in minimum bias carbon-nucleus interactions at beam kinetic energies of 4.0 AGeV and 4.5 AGeV. The results are compared with DCM-SMM, UrQMD, PHSD models of nucleus-nucleus interactions and with the results of other experiments studied carbon-carbon interactions at lower energies.

The Λ hyperon cross sections were evaluated to be $(47.3 \pm 5.8$ mb) and $(52.5 \pm 9.7$ mb) for carbon-carbon collisions at energies of 4.0 AGeV and 4.5 AGeV, respectively. These values are about twice those measured in the propane chamber at energies of 3.36 AGeV (24 ± 6 mb), showing a general increase in cross section with increasing energy. The cross sections and yields of Λ hyperons in the $C + Al$, $C + Cu$, and $C + Pb$ (only for 4.5 AGeV) collisions are presented in Tables 1 and 2 for both beam energies and in Fig. 8. Due to the limited kinematic conditions and set of target nuclei, it is not possible at this time to make a direct comparison with other experiments, as similar data are not available.

The BM@N results for Λ production in $C + C$ collisions at 4.0 AGeV and 4.5 AGeV show good agreement with a proton-proton based parameterization model scaled to the carbon-carbon system. The scaling takes into account the number of participants involved in reaction estimated by the DCM-SMM model as well as isospin effects. This comparison is shown in Figure 9.

In the studied energy ranges the differences between the experimental temperature measurements are not large within the uncertainty values. The temperature increases with increasing atomic number of the target nucleus within the uncertainty limits. For more accurate determination of the temperature dependence it is important to continue such experimental studies.

Acknowledgments BM@N Collaboration gratefully acknowledges the support of BM@N DAQ Cluster Team for providing the necessary resources and facilities that contributed to this research.

References

[1] Exploring strongly interacting matter at high densities - NICA White Paper, Eur.Phys.J. A52 (2016).

[2] BM@N Conceptual Design Report: `http://nica.jinr.ru/files/BM@N/BMN_CDR.pdf`

[3] M. Kapishin (for the BM@N Collaboration), Eur.Phys.J. A52 (2016) no.8, 213.

[4] M. Merschmeyer *et al.* (FOPI Collaboration), K^0 and Λ production in Ni+Ni collisions near threshold, *Phys. Rev. C* **76**, 024906 (2007), arXiv:nucl-ex/0703036

[5] G. Agakishiev *et al.* (HADES Collaboration), Hyperon production in Ar+KCl collisions at 1.76A GeV, Phys. Rev. C **82**, 044907 (2010), arXiv:1010.1675 [nucl-ex].

[6] L. Adamczyk *et al.* (STAR Collaboration), Global Λ hyperon polarization in nuclear collisions: evidence for the most vortical fluid, Nature **548**, 62–65 (2017), doi:10.1038/nature23004.

[7] S. Acharya *et al.* (ALICE Collaboration), Global polarization of Λ and $\overline{\Lambda}$ hyperons in Pb–Pb collisions at $\sqrt{s_{NN}}$ = 2.76 and 5.02 TeV, Phys. Rev. C **101**, 044611 (2020), arXiv:1909.01281 [nucl-ex].

[8] The BM@N collaboration: S. Afanasiev, G. Agakishiev, E. Aleksandrov, I. Aleksandrov, P. Alekseev, K. Alishina, E. Atkin, T. Aushev, V. Babkin, N. Balashov, A. Baranov, A. Baranov et al. Production of pi+ and K+ mesons in argon-nucleus interactions at 3.2 AGeV. Journal of High Energy Physics. – Vol. 7. - 2023. P.174.

[9] BM@N project: `https://bmn.jinr.int/detector/project/BMN_project.pdf`

[10] The BM@N collaboration: S. Afanasiev, G. Agakishiev, E. Aleksandrov, I. Aleksandrov, P. Alekseev, K. Alishina, et al. The BM@N spectrometer at the NICA accelerator complex. Nuclear Instruments and Methods in Physics Research Section A: Accelerators, Spectrometers, Detectors and Associated Equipment - Vol. 1065. – 2024. – P. 169 – 532.

[11] D. Baranov et al., JINST 12 (2017) no.06, C06041.

[12] M. Kapishin (for the BM@N Collaboration), Phys.Atom.Nucl. 80 (2017) no.10, 1613-1619, Yad.Fiz. 7 (2016) no.6, 543-550.

[13] M. Kapishin (for the BM@N Collaboration), Nucl.Phys. A982 (2019) 967-970.

[14] M. Kapishin (for the BM@N Collaboration), Nucl.Phys. A982 (2019) 967-970.

[15] V. Akishina and I. Kisel, J. Phys.: Conf. Ser. 599, 012024 (2015), I. Kisel, Nucl. Instrum. Meth. A **566**, 85 (2006).

[16] B. Friman, W. Nörenberg, and V.D. Toneev, Eur. Phys. J. A **3** (1998).

[17] C. Blume, J. Phys. G **31**, S57 (2005).

[18] A. Andronic *et al.*, Phys. Lett. B **695**, 203 (2011).

[19] N. Amelin, K. Gudima, and V. Toneev, Sov.J.Nucl. Phys. 51, 1093 (1990).

[20] M. Baznat, A. Botvina, G. Musulmanbekov, V. Toneev, V. Zhezher, Phys.Part.Nucl.Lett. 17 (2020) no.3; arXiv: 1912.09277v.

[21] CERN Program Library, Long Writeup W5013, Geneva, CERN, 1993.

[22] `https://git.jinr.ru/nica/bmnroot`

[23] `http://garfieldpp.web.cern.ch/garfieldpp`

[24] D. Baranov et al., Phys.Part.Nucl.Lett. 15 (2018) no.2, 148-156.

[25] K.A. Alishina, Y.Y. Stepanenko, Study of Λ Hyperon Production in Collisions of Heavy Ions with Solid Targets in the BM@N Experiment. Phys. Part. Nuclei Lett. – Vol. 21. – 2024. – P. 683–686.

[26] S.A. Bass *et al.*, Prog. Part. Nucl. Phys. 41 225 (1998).

[27] E.Bratkovskaya *et al.*, PSHD model

[28] H. Angelov et al., P1-80-473, JINR, Dubna.

[29] S. Arakelian et al., P1-83-354, JINR, Dubna.

[30] D. Armutlijsky et al., P1-85-220, JINR, Dubna.

[31] K. Kanaki, PhD: Study of Λ hyperon production in C+C collisions at 2A GeV beam energy with the HADES spectrometer, 2007.

[32] W. Cassing and E. L. Bratkovskaya, "Hadronic and electromagnetic probes of hot and dense nuclear matter," Phys. Rep. 308, 65 (1999).

[33] V.Kolesnikov, V. Kireyeu, V. Lenivenko, A. Mudrokh, K. Shtejer, D. Zinchenko, and E. Bratkovskaya, A New Review of Excitation Functions of Hadron Production in pp Collisions in the NICA Energy Range, PEPAN Letters (2020), Vol. 17, №2, pp. 142-153.

[34] V. Kireyeu, I. Grishmanovskii, V. Kolesnikov, V. Voronyuk, E. Bratkovskaya, Hadron production in elementary nucleon–nucleon reactions from low to ultra-relativistic energies, Eur. Phys. J. A (2020) 56: 223